molecular human reproduction

Molecular Human Reproduction, 2023, **29(10)**, gaad034
https://doi.org/10.1093/molehr/gaad034
Advance Access Publication Date: September 29, 2023
Original Research

Upregulated TIMP1 facilitates and coordinates myometrial contraction by decreasing collagens and cell adhesive capacity during human labor

Junjie Bao [1,*,†], Xiaodi Wang[1,†], Lina Chen[1], Bolun Wen [1], Qiu Gao[2], Xiuyu Pan[1], Yunshan Chen[1], Kaiyuan Ji[1], and Huishu Liu [1,*]

[1]Guangzhou Key Laboratory of Maternal-Fetal Medicine, Department of Obstetrics and Gynecology, Guangzhou Women & Children's Medical Center, Guangzhou Medical University, Guangzhou, China
[2]Department of Pathology, Guangzhou Women & Children's Medical Center, Guangzhou Medical University, Guangzhou, China

*Correspondence address. Guangzhou Key Laboratory of Maternal-Fetal Medicine, Department of Obstetrics and Gynecology, Guangzhou Women & Children's Medical Center, Guangzhou Medical University, Guangzhou 510623, China. E-mail: junjiebaogz@163.com https://orcid.org/0000-0003-3391-8478 (J.B.); Guangzhou Key Laboratory of Maternal-Fetal Medicine, Department of Obstetrics and Gynecology, Guangzhou Women & Children's Medical Center, Guangzhou Medical University, Guangzhou 510623, China. E-mail: huishuliu@hotmail.com https://orcid.org/0000-0002-1197-5343 (H.L.)

†These authors contributed equally to this work.

ABSTRACT

Myometrial contraction is one of the key events involved in parturition. Increasing evidence suggests the importance of the extracellular matrix (ECM) in this process, in addition to the functional role of myometrial smooth muscle cells, and our previous study identified an upregulated tissue inhibitor of metalloproteinase 1 (TIMP1) in human laboring myometrium compared to nonlabor samples. This study aimed to further explore the potential role of TIMP1 in myometrial contraction. First, we confirmed increased myometrial TIMP1 levels in labor and during labor with cervical dilation using transcriptomic and proteomic analyses, followed by real-time PCR, western blotting, and immunohistochemistry. Then, a cell contraction assay was performed to verify the decreased contractility after TIMP1 knockdown *in vitro*. To further understand the underlying mechanism, we used RNA-sequencing analysis to reveal the upregulated genes after TIMP1 knockdown; these genes were enriched in collagen fibril organization, cell adhesion, and ECM organization. Subsequently, a human matrix metalloproteinase (MMP) array and collagen staining were performed to determine the TIMPs, MMPs and collagens in laboring and nonlabor myometrium. A real-time cell adhesion assay was used to detect cell adhesive capacity. The results showed upregulated MMP8 and MMP9, downregulated collagens, and attenuated cell adhesive capacity in laboring myometrium, while lower MMP levels and higher collagen levels and cell adhesive capacity were observed in nonlabor. Moreover, TIMP1 knockdown led to restoration of cell adhesive capacity. Together, these results indicate that upregulated TIMP1 during labor facilitates and coordinates myometrial contraction by decreasing collagen and cell adhesive capacity, which may provide effective strategies for the regulation of myometrial contraction.

Keywords: tissue inhibitor of metalloproteinase 1 / matrix metalloproteinase / myometrial smooth muscle cell / contraction / collagen / adhesion / extracellular matrix

Introduction

Parturition is a well-orchestrated physiological process characterized by cervical ripening, increased myometrial contraction, fetal membrane rupture, and placental separation (Khader *et al.*, 2021; Pique-Regi *et al.*, 2022). Myometrial contraction is one of the most important events in this process. Functional withdrawal of progesterone, inflammation, mechanical stretch, and hypoxia all contribute to myometrial contraction (Nadeem *et al.*, 2016; Chen *et al.*, 2021; Li *et al.*, 2021; Wen *et al.*, 2022; Barnett *et al.*, 2023), while the states of contraction are controlled by electrical activity of human myometrial smooth muscle cells (hMSMCs) (Rabotti and Mischi, 2015; Lucovnik *et al.*, 2018; Ma *et al.*, 2020).

The extracellular matrix (ECM), as a structural and biochemical support to surrounding cells, has recently been suggested to regulate myometrial contraction by remodeling (Lombardi *et al.*, 2018; Fan *et al.*, 2020; Ouellette *et al.*, 2022). Tissue inhibitor of metalloproteinase 1 (TIMP1), which participates in regulating proteolysis of matrix metalloproteinase (MMP)-dependent ECM (Arpino *et al.*, 2015), was found to be upregulated in human laboring myometrium in our previous study (Chen *et al.*, 2021). However, its role in laboring has not yet been fully elucidated.

TIMP1 is a glycoprotein of the TIMP family, which includes four TIMPs (TIMP1–4) that have similar but not identical protease inhibitory profiles (Stetler-Stevenson, 2008). TIMP1 is constitutively expressed in most normal tissues, including the uterus, ovaries, brain, heart, liver, and arteries. This molecule can be induced on the surface of some cells as membrane-bound forms and/or be secreted by the majority of the body's cells as soluble forms (Cabral-Pacheco *et al.*, 2020). Recent evidence reveals that TIMP1 is a multifunctional protein with pleiotropic activities (Arpino *et al.*, 2015). Generally, it is believed to directly inhibit

Received: March 24, 2023. **Revised:** September 11, 2023. **Editorial decision:** September 27, 2023.

MMPs, a disintegrin and metalloproteinases (ADAMs), and ADAMs with thrombospondin motifs and thereby regulate ECM proteolysis and matrix remodeling during pregnancy, parturition, and postpartum (Baker *et al.*, 2002; Geng *et al.*, 2016). However, TIMP1 was also reported to indirectly inhibit the release of TGF-β activated by MMPs (Yu and Stamenkovic, 2000) and result in decreased ECM deposition (Noble *et al.*, 1992); it could restrict both inflammation and ECM accumulation/fibrosis in liver and lung injury mice (Kim *et al.*, 2005; Wang *et al.*, 2011; Arpino *et al.*, 2015) and could also facilitate proteolysis around neutrophils by anchoring matrix MMP8 and MMP9 to the surface of neutrophils. The divergent roles of TIMP1 may depend on the specific tissue environment (Wang *et al.*, 2019).

Since TIMP1 is expressed in the myometrium of essentially all species (Nothnick, 2000; Nguyen *et al.*, 2016; Lombardi *et al.*, 2018) and our previously established myometrial transcriptome and proteome data (Chen *et al.*, 2021) revealed the upregulated expression of TIMP1 in human laboring myometrium, our present study aims to explore the potential role of TIMP1. First, to identify its relationship with the progression of labor, we determined that myometrial TIMP1 levels continuously increased in labor and during labor with continuous cervical dilation. Then, an *ex vivo* cell contraction assay was performed to verify decreased contractility after TIMP1 knockdown in hMSMCs. Next, RNA-seq analysis before and after TIMP1 knockdown was used to explore the potential mechanism underlying it, followed by a series of experiments, including an MMP array, collagen staining, and a real-time cell adhesion assay to further confirm these findings.

Materials and methods

Human myometrium

Human myometrial samples without serosa and endometrium from the lower uterine segment were collected from 20 to 40 years old, nulliparous women with a singleton pregnancy undergoing elective or emergency cesarean section in Guangzhou Women and Children's Medical Center. Regular contractions (<3 min apart) and progressive dilatation of the cervix (>2 cm) were defined as labor. The surgical indication was breech presentation, cephalopelvic disproportion, or fetal distress. Non-pregnant biopsies were obtained from the corresponding area of the normal uterus at hysterectomy. Women with any of the following conditions were excluded: (i) complications, including hypertension, eclampsia, cholestasis, gestational diabetes, and other diseases; (ii) abnormal labor, including uterine atony or prolonged labor; (iii) placental abnormality, including placental abruption and placenta previa; and (iv) infectious diseases. Detailed information on the subjects is provided in Supplementary Table S1. All subjects signed written consent forms approved by the ethics committee of Guangzhou Women and Children's Medical Center (approval no. 201915401&2023036A01).

Isolation and culture of hMSMCs

As we described before (Wen *et al.*, 2022), myometrial tissue was cut into tiny pieces with visible blood vessels removed after washing twice in PBS. Explants were cultured in DMEM (Dulbecco's modified eagle medium, C11995500BT, Gibco, Grand Island, NY, USA) with 10% (v/v) fetal bovine serum (FBS) (#10099-141, Gibco, Grand Island, NY, USA) and 1% penicillin–streptomycin (#15140122, Gibco, Grand Island, NY, USA) for 2 weeks at 37°C with 5% CO_2 in air. Then, the cells were harvested and further subcultured. Caldesmon (CDM) and α-smooth muscle actin (SMA) were used as markers to identify the myometrial smooth muscle cells. Cells were used at passage 1 or 2 in this study.

Cell transfection and infection

TIMP1 in hMSMCs was silenced with siRNA (si-TIMP1, 10 nM) (IGEbio, Guangzhou, China) or si-NC as a negative control when cells reached 70–80% confluency using Rfect reagent (INTERFERin®, 409-10, Polyplus, Strasbourg, France). The sense and antisense sequences were as follows: si-TIMP1 (F: 5′-ACAGACGGCCUUCUGCAAUUC-3′; R: 5′-GAAUUGCAGAAGGCCG UCUGU-3′) si-NC, (F: 5′-UUCUCCGAACGUGUCACGU-3′; R: 5-AC GUGACACGUUCGGAGAA-3′).

TIMP1 in hMSMCs was overexpressed with TIMP1 overexpression lentiviral particles (oe-TIMP1) (Genechem, Shanghai, China). The oe-TIMP1 lentiviruses were constructed using the lentiviral vector GV358 with a green fluorescent protein reporter and TIMP1 CDS (Genechem, Shanghai, China). Fluorescence microscopy was used to confirm the efficiency of infection.

Cells were collected for subsequent experiments 24–72 h after infection or transfection.

Real-time PCR

An RNeasy mini kit (#74104, Qiagen, Hilden, Germany) was used to extract total RNA. Then, RNA was reverse transcribed using the PrimeScript™ RT reagent Kit with gDNA Eraser (RR047B, TaKaRa, Otsu, Shiga, Japan). Real-time PCR was performed using a QuantStudio™ Real-Time PCR System (Applied Biosystems) with TB Green Premix Ex Taq II (Tli RNaseH Plus, RR820L Takara, Otsu, Shiga, Japan). The PCR conditions were as follows: 95°C for 10 min for PCR initial heat activation, 40 cycles of 95°C for 15 s for denaturation and combined annealing/extension at 60°C for 1 min. Samples were run in triplicate using β-actin as an internal control. Data were analyzed using the $2^{-\Delta Ct}$ method.

Western blotting

Protein was extracted from myometrium or hMSMCs. Samples were prepared as previously described (Bao *et al.*, 2016), subjected to 12% sodium dodecyl sulfate–polyacrylamide gel electrophoresis (SDS–PAGE), and then transferred to polyvinylidene fluoride (PVDF) membranes (IPVH07850, Millipore, Darmstadt, Germany). Protein was probed with primary and secondary antibodies, and signals were detected by an ECL chemiluminescence system (#32106, Thermo Scientific, RockFord, IL, USA). β-actin was used in all experiments as a loading control. The antibodies used were rabbit polyclonal β-actin antibody (1:5000, ab8226, Abcam, Cambridge, UK), rabbit monoclonal TIMP1 antibody (1:1000, ab211926, Abcam, Cambridge, UK), rabbit polyclonal NID2 (1:1000, DF9704, Affinity Biosciences, Changzhou, China), rabbit monoclonal VCAN (1:1000, ab270444, Abcam, Cambridge, UK), rabbit polyclonal SPP1 (1:1000, GB112328, Servicebio, Wuhan, China), and rabbit polyclonal GAPDH (1:1000, AF7021, Affinity Biosciences, Changzhou, China).

Immunohistochemistry and immunofluorescence

Myometrial tissue or hMSMCs were fixed and prepared as we described previously (Wen *et al.*, 2022). In brief, sections or cells were incubated with primary antibodies overnight at 4°C after blocking. After washing, a horse radish peroxidase (HRP)-labeled secondary antibody was added for immunohistochemistry, using 3,3′-diaminobenzidine as a chromogenic substrate (G1211,

Servicebio, Wuhan, China), while fluorescently labeled secondary antibodies were used for immunofluorescence. Nuclei were visualized using hematoxylin for immunohistochemistry or DAPI for immunofluorescence. All images were acquired using a Leica DMi8 fluorescence microscope (Leica, Wetzlar, Germany) with Leica Application Suite X software. Analysis of fluorescence intensity was performed using ImageJ (Lv *et al.*, 2021).

The antibodies and kits used in immunostaining were as follows: rabbit monoclonal TIMP1 antibody (1:200, ab211926, Abcam, Cambridge, UK), mouse polyclonal α-SMA (1:300, ab7817, Abcam, Cambridge, UK), rabbit polyclonal collagen I (1:2000, GB11022, Servicebio, Wuhan, China), rabbit polyclonal collagen III (1:1000, GB111629, Servicebio, Wuhan, China), rabbit polyclonal collagen V (1:1500, GB111012, Servicebio, Wuhan, China), goat anti-rabbit Alexa Flour488-IgG (1:500, ab150077, Abcam, Cambridge, UK), goat anti-mouse Alexa Flour647-IgG (1:500, ab150115, Abcam, Cambridge, UK), goat anti-rabbit IgG H&L HRP (1:2000, ab205718, Abcam, Cambridge, UK), and goat anti-mouse/rabbit multiplex IFC detection kit (#18003, Zenbio, Chengdu, China).

Cell contraction assay

The contractility of hMSMCs was evaluated by a cell contraction assay kit (CBA-201, Cell Biolabs, Inc., San Diego, CA, USA). The cells were trypsinized and suspended, and the collagen solution was diluted with DMEM to a final concentration of 1.0 mg/ml. The cells and collagen solution were then mixed and plated into a 24-well plate (1.5×10^5 cells/well) for 1 h at 37°C. After the gel was polymerized, a volume of 1.0 ml of DMEM with 10% FBS was added to each well and cultured for 24 h. Then, the medium was replaced, and the gels were released from the well sides. Gels were imaged at 2 h using a ChemiDoc XRS+ system (Bio-Rad, Hercules, CA, USA), and the area of gel lattices was measured using ImageJ software (National Institutes of Health, Bethesda, Maryland, USA). BDM (2,3-butanedione monoxime) was used as a contractile inhibitor.

RNA sequencing (RNA-seq) and data analysis

A RNA-seq library was generated by the VAHTS Universal V6 RNA-seq library preparation kit for Illumina (San Diego, CA, USA; NR604-01/02). In brief, mRNA was purified and then fragmented with fragmentation buffer. First- and second-strand cDNAs were synthesized. The end of the double strand cDNA was repaired, a tail was added, and the sequencing linker was connected. The final cDNA library was obtained by PCR amplification. The RNA concentration of the library was quantified preliminarily using a Qubit RNA analysis kit in Qubit 3.0. The insert size was assessed using an Agilent Bioanalyzer 2100 system (Agilent Technologies, Santa Clara, CA, USA). The effective concentration was determined accurately by qPCR. Paired-end sequencing was performed on the Illumina HiSeq system. The raw data can be obtained from the Genome Sequence Archive (GSA) (https://ngdc.cncb.ac.cn/gsa-human/browse/HRA003324).

RNA-seq reads were mapped to the genome (*Homo sapiens*, GRCh38) and transcriptome using hisat2. The read counts were calculated, and the readings were assigned to Ensemble gene annotations (*H. sapiens*, release 84). The differentially expressed mRNAs in the two groups were identified using the DEseq2 package in R (v4.1.1). Gene Ontology (GO) annotation and Kyoto Encyclopedia of Genes and Genomes (KEGG) pathways were enriched by DAVID (v6.8). Gene set enrichment analysis (GSEA) was performed using GSEA implementation based on the molecular signatures database (MsigDB) gene sets, and a false discovery rate <0.05 was considered significant.

Human MMP protein array

Levels of TIMPs and MMPs were determined using the RayBio Human Matrix Metalloproteinase Antibody Array (AAH-MMP-1-2, RayBiotech, Norcross, GA, USA), which permitted the measurement of MMP-1–3, -8, -9, -10, and -13 and of TIMP1, 2, and 4 in a single procedure. In brief, each membrane was placed into a well of the incubation tray, and diluted tissue lysates of 500 μg total protein or cell culture media were loaded into each well and then incubated overnight at 4°C. After two-step washes, biotinylated antibody was added and incubated overnight at 4°C. Then, the wells were washed again, and HRP-labeled streptavidin was added, which could combine with biotin to produce signals for chemiluminescence detection. Analysis was performed using ImageJ.

Real-time cell adhesion assay

Experiments were carried out using an RTCA S16 xCELLigence instrument (Agilent Technologies, Santa Clara, CA, USA), which measures cell adherence to the bottom of the well through microelectronic biosensors and translates signals into a relative cell index. The instrument was in a humidified incubator maintained at 37°C with 5% CO_2. For adhesion, control cells and conditioned cells were seeded in 16-E-plates at 5000 cells/well in medium containing 10% FBS. Plates were monitored once every 10 min for a total of 6 h to evaluate the cell adhesive capacity. Data were acquired using RTCA software Version 1.2 and exported for statistical analysis.

Statistical analysis

Data are presented as means ± SEM and were analyzed by GraphPad Prism 8.4.0 software (San Diego, CA, USA). After normality tests, *t* tests (and nonparametric tests) were used for comparisons of two groups, and ANOVA (and nonparametric or mixed tests) was used for comparisons of multiple groups. A *P*-value ≤0.05 was considered to be statistically significant.

Results

TIMP1 is upregulated in human laboring myometrium

TIMP1 was upregulated in human laboring myometrium compared to nonlabor myometrium at both the protein and mRNA levels ($P = 0.015$, $P < 0.001$, respectively), based on analysis of the myometrial transcriptome and proteome data from our previous study (Fig. 1A–C, where Fig. 1A was adapted from our previous work) (Chen *et al.*, 2021). This was further verified by real-time PCR and western blotting (Fig. 1D and E). The mRNA expression of other TIMPs and MMPs in human in-labor (IL) and nonlabor (NL) myometrium is also presented in a heatmap (Fig. 1B).

TIMP1 continues to increase with continuous cervical dilation during labor

The trend of TIMP1 expression during labor was subsequently analyzed based on the clinical data, which recorded the degree of cervical dilation at the moment of cesarean section. The mRNA level of TIMP1 increased with continuous cervical dilation ($r = 0.783$, $P = 0.007$, Fig. 2A), and the immunohistochemistry results also showed enhanced and increased positive staining of TIMP1 from cervical dilations of 2 cm and 4 cm to 8 cm (Fig. 2B).

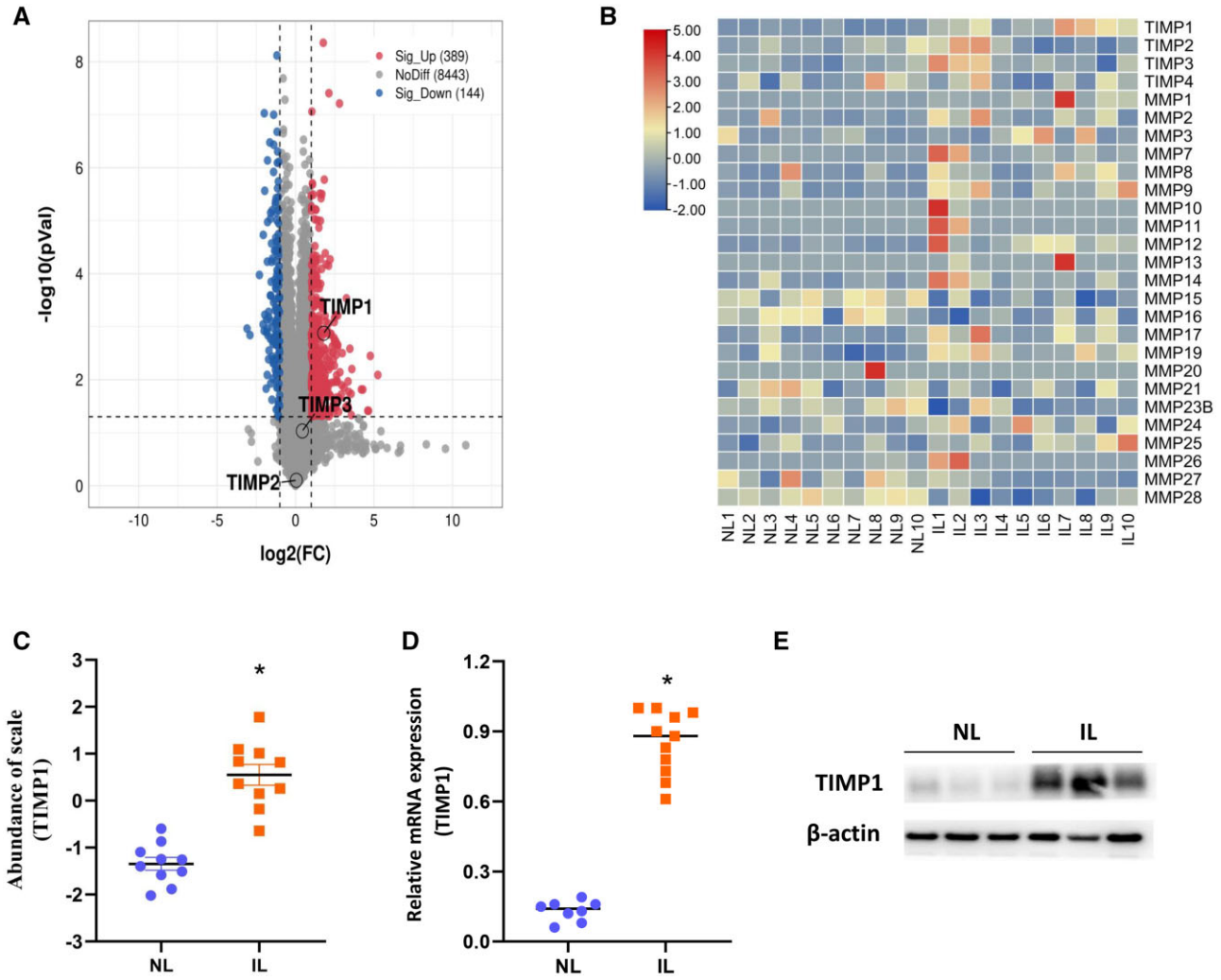

Figure 1. Expression of tissue inhibitor of metalloproteinase 1 (TIMP1) in human inlabor (IL) and nonlabor (NL) myometrium. (**A**) Volcano plot of all mRNA alterations in human IL myometrium compared to NL myometrium, adapted from our previous work (Chen *et al.*, 2021). The horizontal dashed line corresponds to $P < 0.05$, and the vertical line corresponds to a 1.5-fold decrease or increase in expression levels. Red, blue, and gray dots represent upregulated, downregulated, and non-differentially expressed transcripts, respectively, in the IL group compared to the NL group. (**B**) Heatmap of the mRNA expression of TIMPs and MMPs in human IL and NL myometrium. (**C**) Protein expression of TIMP1 (26 kDa) in human IL and NL myometrium by Parallel Reaction Monitoring (PRM). (**D**) Relative mRNA expression of TIMP1 in human IL and NL myometrium by real-time PCR. (**E**) Protein expression of TIMP1 in human IL and NL myometrium by western blotting. See Supplementary Fig. S1 for full western blots. Data are presented as mean ± SEM from 3 to 10 independent experiments. *$P < 0.05$.

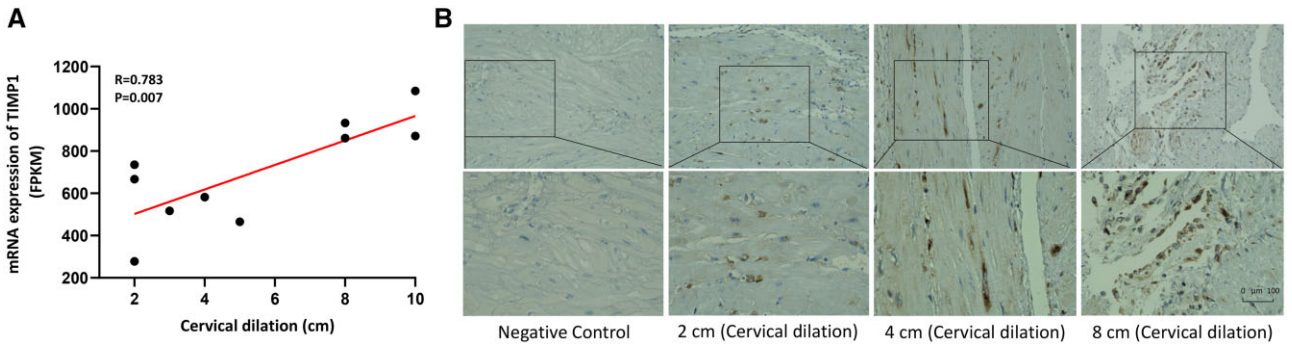

Figure 2. Tissue inhibitor of metalloproteinase 1 (TIMP1) expression in myometrium during the progression of labor. (**A**) The mRNA expression of TIMP1 with persistent cervical dilation during labor. (**B**) The protein expression of TIMP1 at different stages of cervical dilation. TIMP1.

Knockdown of TIMP1 damages the contractile function of hMSMCs

Knockdown of TIMP1 was validated by immunofluorescence, real-time PCR and western blotting (Fig. 3A–C). Results from a cell contraction assay showed a decreased gel reduction area in the si-TIMP1 cells compared to the control cells, si-NC cells, and BDM-treated cells ($P = 0.004$, $P = 0.002$, $P < 0.001$, respectively), which indicated a decreased contractile function of TIMP1 knockdown cells (Fig. 3D and E).

Gene alteration after TIMP1 knockdown is associated with collagen fibril organization and cell adhesion

To reveal the mechanism underlying the TIMP1-dependent contractile function of hMSMCs, we performed RNA-seq analysis before and after TIMP1 knockdown. Gene alterations are presented in a volcano plot (Fig. 4A), with 49 upregulated and 49 downregulated genes after TIMP1 knockdown. Functional enrichment analysis showed some enriched biological processes, including focal adhesion and ECM-receptor interaction (Fig. 4B). The GO analysis suggested that most upregulated genes were enriched in collagen fibril organization, cell adhesion, and ECM organization, while most downregulated genes were involved in the innate immune response (Fig. 4C). Gene set enrichment analysis (GSEA) detailed the enrichment of ECM-receptor interactions and cell adhesion in the si-TIMP1 cells (Fig. 4D).

Increased expression of MMP8, MMP9, and TIMP1 along with degraded collagens in the laboring myometrium

A human MMP array was performed to detect TIMPs and MMPs in human laboring and nonlabor term myometrium, and immunofluorescence staining was performed to show the possible changes in collagen I, III, and V (the predominant collagens in myometrium) since the TIMP: MMP system is the main group responsible for collagen and other degradation in ECM. The results showed significant increases in MMP8, MMP9, and TIMP1 in the

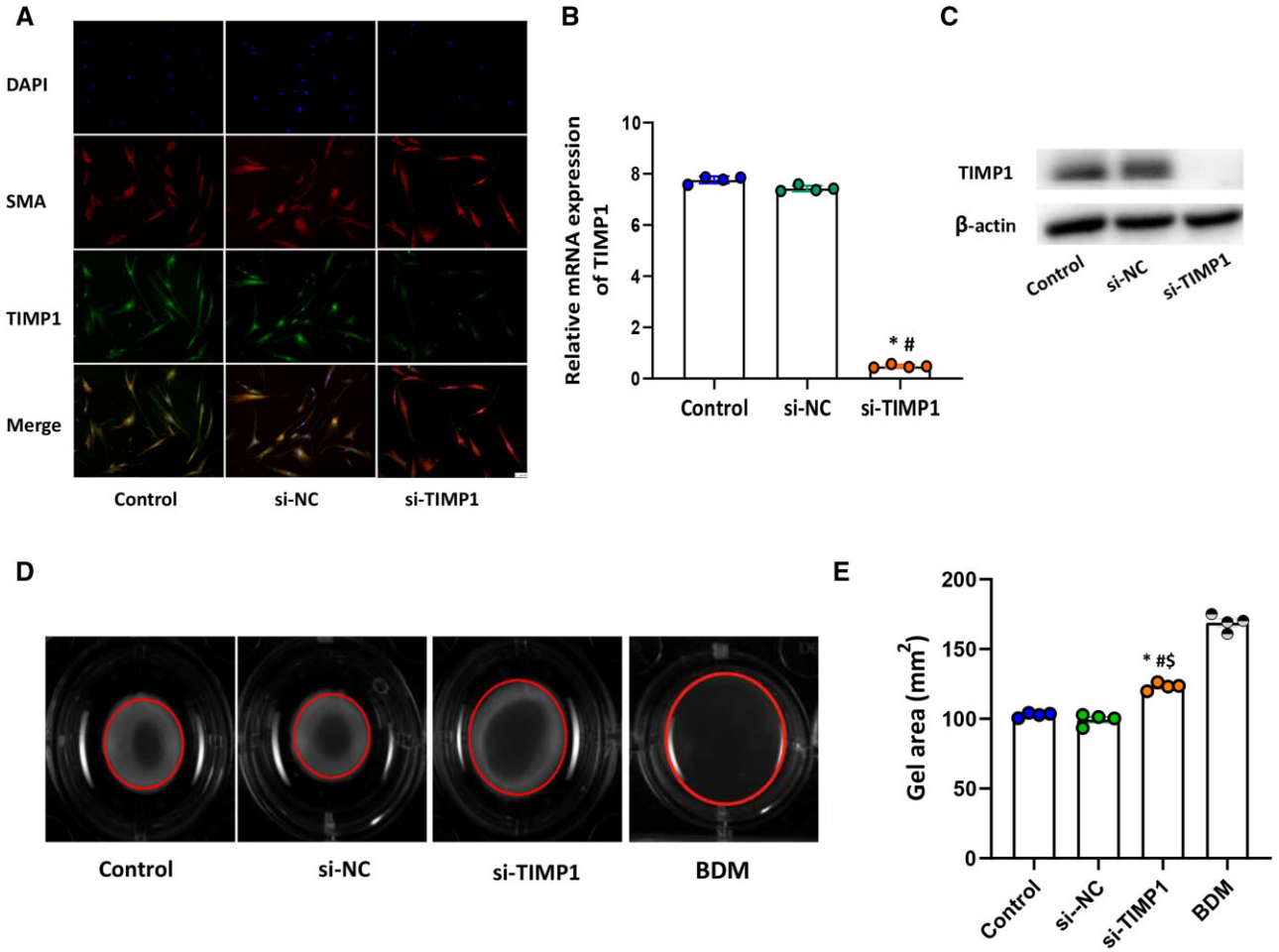

Figure 3. Effect of tissue inhibitor of metalloproteinase 1 (TIMP1) knockdown on the contractility of human myometrial smooth muscle cells (hMSMCs) *in vitro*. (**A**) Immunofluorescence staining of TIMP1 in control hMSMCs and cells transfected with si-NC or si-TIMP1. (**B**) Relative mRNA expression of TIMP1 detected by real-time PCR. (**C**) Protein expression of TIMP1 (26 kDa) detected by western blotting. See Supplementary Fig. S2 for full western blots. (**D**) Contractility assessment of hMSMCs with/without TIMP1 knockdown using a cell contraction assay. BDM (2,3-butanedione monoxime, a cell contraction inhibitor) was used as a contractile inhibitory control. (**E**) Gel area calculation of hMSMCs with/without TIMP1 knockdown. Data are presented as mean ± SEM from 3 to 4 independent experiments. *si-TIMP1 versus the control, $P < 0.05$; #si-TIMP1 versus si-NC, $P < 0.05$; $si-TIMP1 versus BDM, $P < 0.05$.

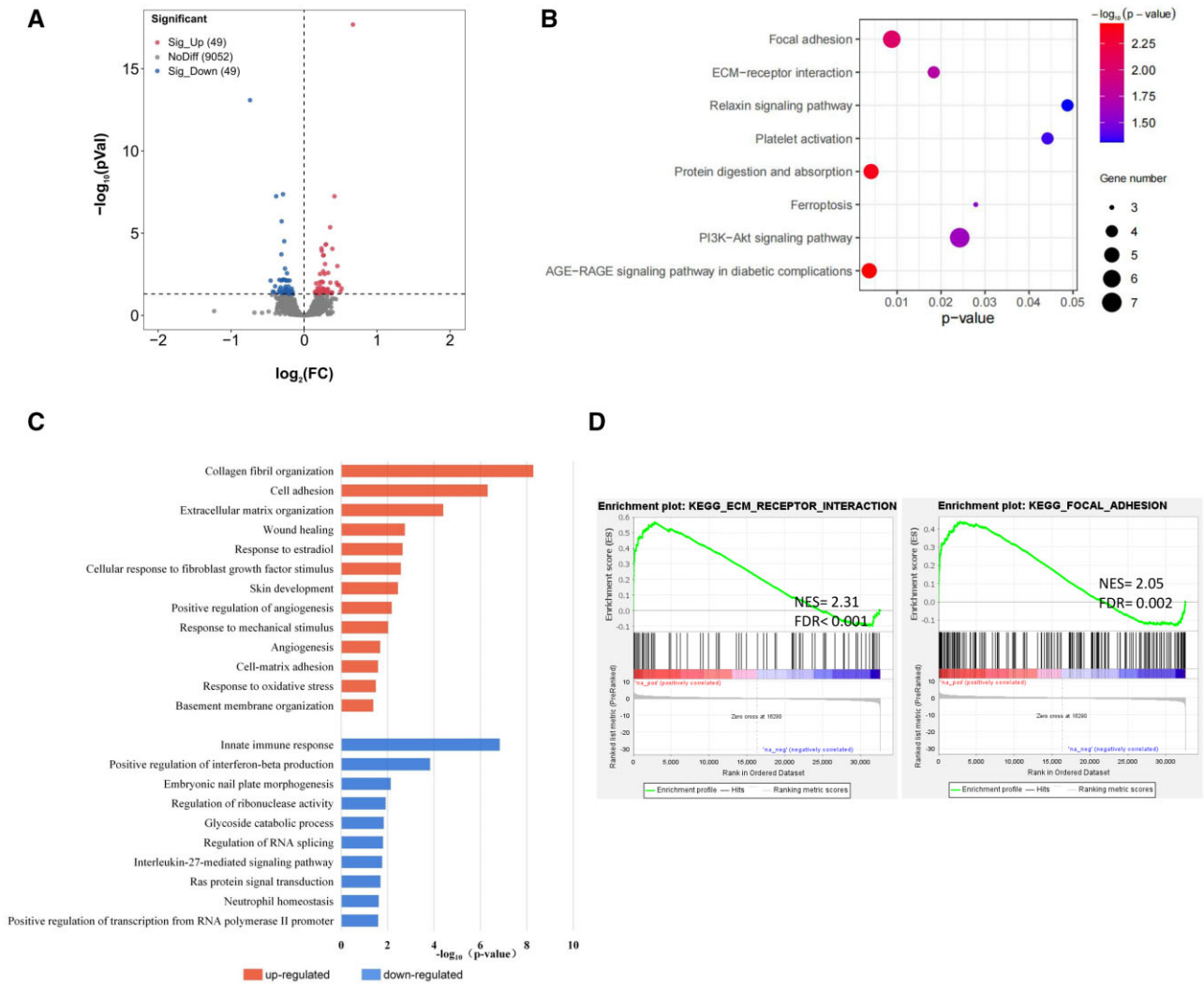

Figure 4. Visualization of the transcriptomics results after knockdown of tissue inhibitor of metalloproteinase 1 (TIMP1). (**A**) Volcano plot of gene alterations. (**B**) Bubble diagram showing partial significantly enriched pathways. (**C**) Bar diagram showing partial biological progress Gene Ontology (GO) term clusters. Red and blue represent upregulated and downregulated pathways, respectively. (**D**) Gene set enrichment analysis (GSEA) plots of extracellular matrix (ECM) receptor interaction and focal adhesion mRNA sets.

laboring myometrium compared to the nonlabor myometrium (Fig. 5A–C, $P = 0.004$, 0.046, and 0.009, respectively), accompanied by degraded collagen I, III, and V (Fig. 5D and E, $P = 0.002$, 0.015, and 0.012, respectively). Merging images in Fig. 5D showed the overall degradation of collagen I, III, and V in the laboring myometrium compared to the nonlabor myometrium. There was also high expression of TIMP2; however, no significant difference was found between the in-labor and nonlabor groups.

Attenuated cell adhesive capacity in laboring hMSMCs and enhanced cell adhesive capacity after TIMP1 knockdown

A real-time cell adhesion assay was performed to assess the cell adhesive capacity in hMSMCs of different statuses. The results showed a decreased cell adhesive index in laboring hMSMCs compared to nonlabor and nonpregnant hMSMCs (Fig. 6A, $P < 0.001$). This attenuated adhesive capacity of laboring cells could be restored after transfection with si-TIMP1 (Fig. 6B, $P < 0.001$), which indicated a substantial relationship between TIMP1 and cell adhesive capacity in laboring.

The adhesive index in cells with oe-TIMP1 was also assessed simultaneously and showed a slight downward trend compared to that of the control group but with no significant difference (Fig. 6B, $P = 0.177$).

In addition, some essential proteins were detected to further verify the effect of TIMP1 on cell adhesion by western blotting. There was increased osteopontin (SPP1) and nidogen-2 (NID2) expression in the si-TIMP1 cells compared to the control cells, with a slight upward trend of versican (VCAN) (Fig. 6C and D, $P = 0.003$, 0.042, and 0.414, respectively), which was consistent with the results from RNA-seq analysis before and after TIMP1 knockdown (Fig. 6E, $P = 0.019$, $P < 0.001$, and $P < 0.001$, respectively).

Discussion

Myometrial contraction is a complex event during labor requiring the coordination of multiple factors. In this study, we observed increased myometrial TIMP1 in labor and during labor with cervical dilation, which suggested a relationship between TIMP1 and myometrial contraction. Cell contraction assays further verified decreased contractility after TIMP1 knockdown *in vitro*, and the results from RNA sequencing revealed that the upregulated genes after TIMP1 knockdown were enriched in collagen fibril organization and cell adhesion. The increased MMP8 and MMP9,

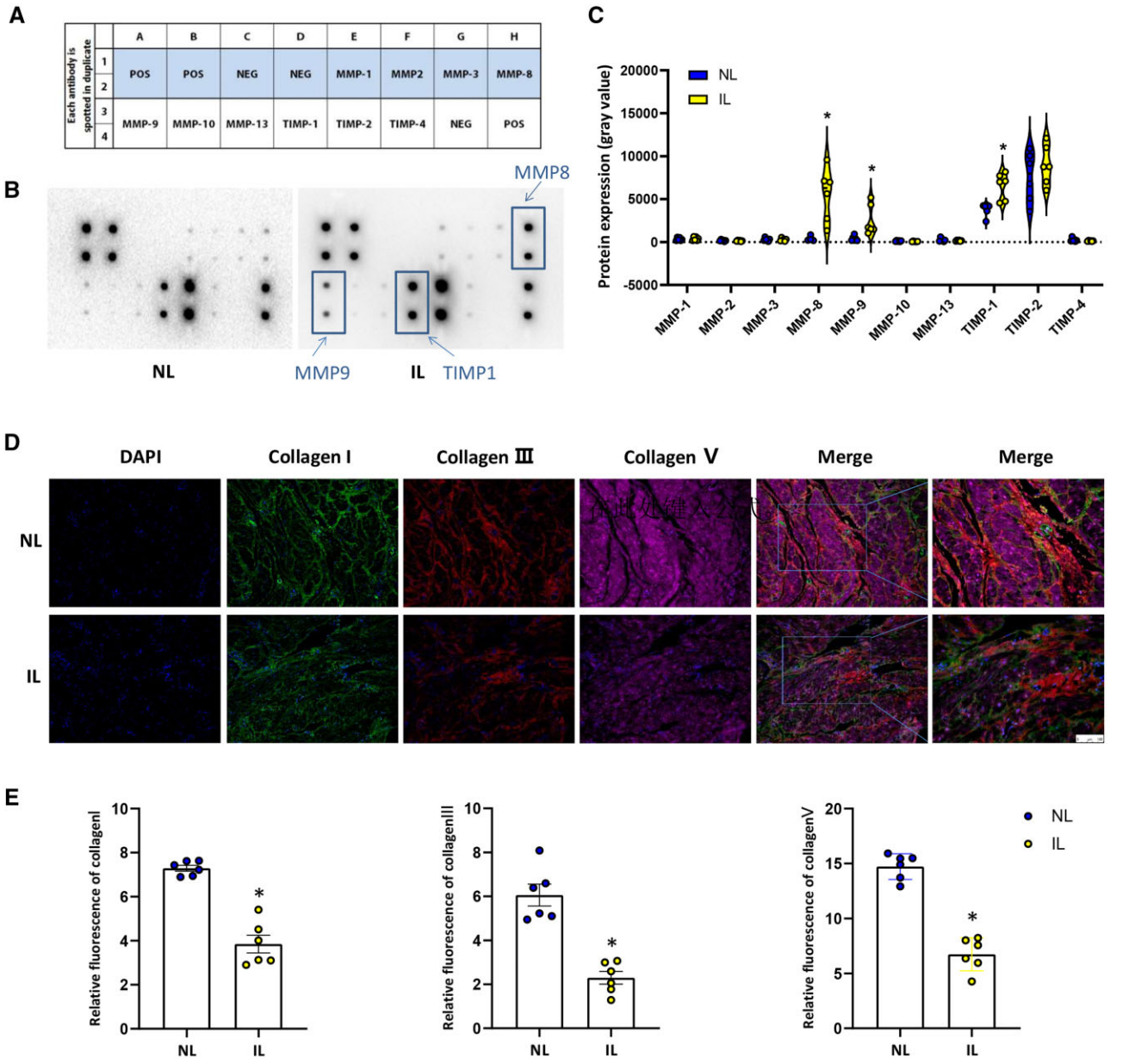

Figure 5. Changes of tissue inhibitor of metalloproteinases (TIMPs) matrix metalloproteinases (MMPs) and collagens in human laboring myometrium. (**A**) Template showing the location of the TIMP and MMP antibodies spotted onto the RayBiotech human MMP array kit. POS: positive; NEG: negative. (**B**) Human MMP array shows the protein expression of TIMPs and MMPs in human inlabor (IL) and nonlabor (NL) myometrium. Blue boxes are used to highlight the upregulated MMP8, MMP9 and TIMP1 in human IL myometrium. See Supplementary Fig. S3 for all the human MMP array results. (**C**) Analyses of gray values from the human MMP array by ImageJ. (**D**) Immunofluorescence staining shows the differential expression of collagen I, III and V in human IL and NL myometrium. Scale bar = 100 μm. (**E**) Fluorescence intensity of collagen I, III, and V in human IL and NL myometrium. Data are presented as mean ± SEM from 6 independent experiments. *$P < 0.05$.

degraded collagens, and attenuated adhesive capacity of hMSMCs were subsequently demonstrated in laboring myometrium compared to nonlabor samples, while enhanced cell adhesive capacity and damaged contractile function were found with TIMP1 knockdown, which further validated that TIMP1 may facilitate and coordinate human myometrial contraction by decreasing collagens and cell adhesive capacity. The current study provided a plausible explanation for the increase in myometrial TIMP1 with the progression of labor.

TIMP1, as an important regulator of MMP-dependent ECM, has been investigated in many tissues of different species (Arpino *et al.*, 2015; Prideaux *et al.*, 2015), including the myometrium of mice, rats, and humans (Nguyen *et al.*, 2016; Lombardi *et al.*, 2018). However, our study is the first, to our knowledge, to report that myometrial TIMP1 continued to increase with the progression of labor and that knockdown of TIMP1 could impair the contractile function of hMSMCs. These results confirmed the relationship between TIMP1 and myometrial contraction.

Increasing evidence shows the importance of the ECM as well as cells in tissues. As an extensive molecular network in which cells reside, the ECM provides support and anchorage for cells and regulates cellular functions, such as survival, growth, adhesion, proliferation, migration, and differentiation (Humphrey *et al.*, 2014). The core matrisome is composed of ~300 unique matrix macromolecules and complex ECM remodeling processes involving more than 700 proteins. ECM remodeling is an essential and delicately regulated physiological process. Constant ECM remodeling supports the dramatic growth of the uterus during

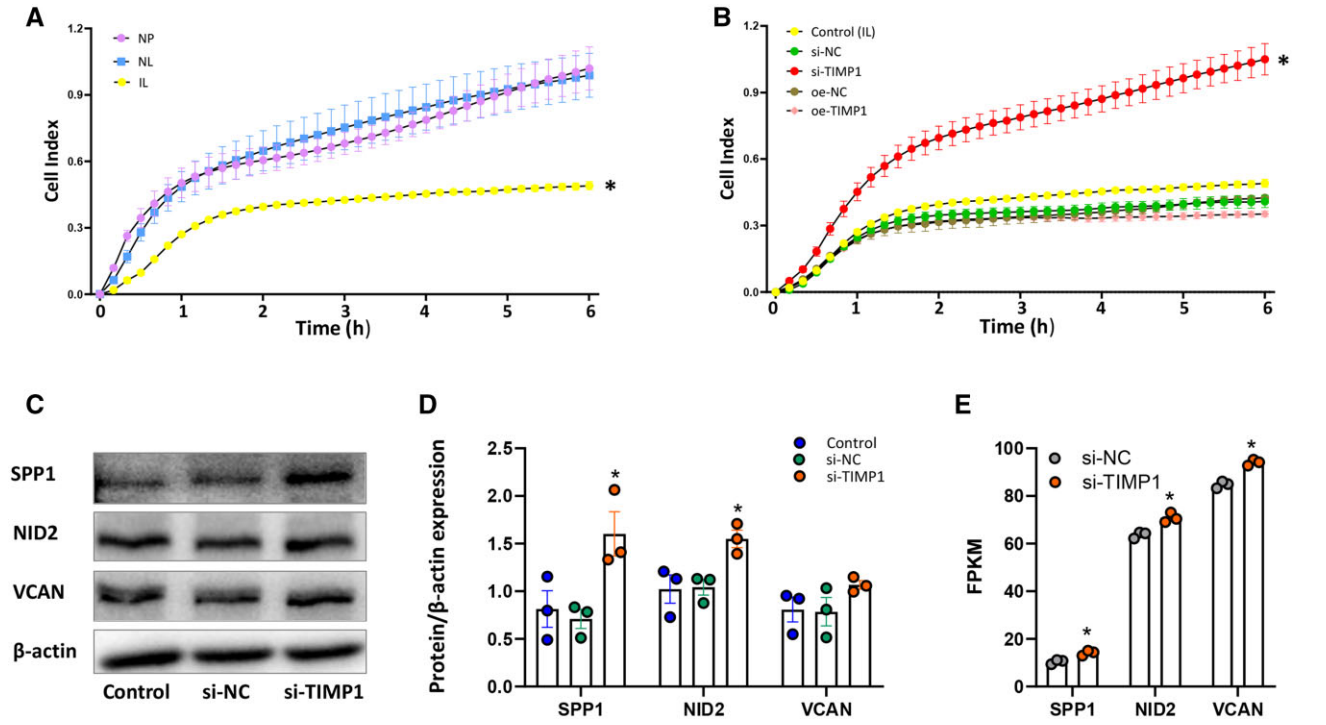

Figure 6. Different cell adhesive properties in different human myometrial smooth muscle cells (hMSMCs). (**A**) Cell adhesive properties in nonpregnant, nonlabor and in-labor term hMSMCs. *IL versus NL, $P < 0.05$. (**B**) Cell adhesion properties in laboring hMSMCs with/without si-TIMP1 or oe-TIMP1. *si-TIMP1 versus the control, $P < 0.05$. (**C**) Representative western blotting of SPP1 (70 kDa), NID2 (151 kDa), and VCAN (373 kDa) in laboring hMSMCs with/without si-TIMP1 knockdown. See Supplementary Fig. S4 for full western blots. (**D**) Ratio of SPP1, NID2, and VCAN/β-actin expression in western blotting. (**E**) RNA-seq analysis shows the mRNA expression before and after si-TIMP1 knockdown. TIMP1, tissue inhibitor of metalloproteinase 1; SPP1, osteopontin; NID2, nidogen-2; VCAN, versican; NL, nonlabor; IL, in-labor. Data are presented as mean ± SEM from 3 to 10 independent experiments. *$P < 0.05$.

pregnancy (Stewart *et al.*, 1995). However, it remains unknown whether TIMP1 could facilitate uterine contraction in labor by regulating the ECM. The RNA-seq analysis in the current study identified upregulated genes in collagen fibril organization, cell adhesion and ECM organization after TIMP1 knockdown, which provided the first support for our hypothesis.

ECM proteolysis and remodeling could be regulated by TIMP1 (Arpino *et al.*, 2015) and has been reported to affect the mechanical strength and flexibility of the cervix in its softening, ripening, dilation, and postpartum involution (Read *et al.*, 2007; Oxlund *et al.*, 2010; Timmons *et al.*, 2010). While as the most dynamic organ during pregnancy, parturition, and postpartum, little attention has been given to uterine ECM remodeling.

We observed increasing levels of TIMP1, MMP8, and MMP9 in the laboring myometrium by a protein array. Interestingly, a moderate increase in TIMP1 and a dramatic increase in MMP8 and MMP9 were found to be the most notable changes in the TIMP: MMP system of human laboring myometrium, instead of MMP3 and MMP10, which were reported to increase and decrease in laboring myometrium, respectively (O'Brien *et al.*, 2007; Lombardi *et al.*, 2018). The different results may be due to the different methods and the various samples. The human MMP array used in this study permits more comparable data in one process. The increased ratio of MMPs to TIMPs indicates the disruption of the original balance between TIMPs and MMPs and enhanced ECM proteolysis, which may facilitate uterine contraction in laboring (Manase *et al.*, 2006; Geng *et al.*, 2016).

MMP8 and MMP9 belong to the collagenase subgroup of MMPs. These molecules exist as both soluble forms and membrane-bound forms and serve as the main ECM enzymes in collagen degradation (Bockelman *et al.*, 2018). MMP8, known as neutrophil collagenase, can degrade collagen I–III, V, VII, VIII, and X and other ECM components. MMP9, a gelatinase, can degrade gelatin, collagen IV, V, VII, X, and XIV, and other substrates in the ECM (Jabłońska-Trypuć *et al.*, 2016). Their levels in human laboring myometrium were significantly elevated, which was consistent with previous reports that they both increased in the lower uterine segment during parturition (Winkler *et al.*, 1999a,b). The increased MMP8 is supposed to be secreted by inflammatory cells infiltrated in the myometrium, while MMP9 is from not only inflammatory cells but also hMSMCs (Geng *et al.*, 2016). Membrane-bound MMP8 and MMP9 have been reported to be TIMP-resistant (Owen *et al.*, 2003; Owen *et al.*, 2004), which could partly explain their coexistence with high levels of TIMP1 in the current study. Moreover, a recent study by Owen's team showed that TIMP1 could upregulate membrane-bound MMP8 and MMP9 in polymorphonuclear neutrophils, thereby promoting pericellular proteolysis (Wang *et al.*, 2019). This finding helps to explain not only the elevations of both TIMP1 and MMPs in the laboring myometrium but also the enhanced collagen degradation in the current study. Certainly, this elevation of TIMP1 may also be a feedback response to the dramatic increase in MMP8 and MMP9. Further research is needed to explore this possibility in the human myometrium.

As the predominant collagens in the myometrium (Kao and Leslie, 1977; Jayes *et al.*, 2019) and the regular substrates of MMP8 and MMP9 (Jabłońska-Trypuć *et al.*, 2016), collagen I, III, and V in the myometrium were subsequently investigated. The degradation of collagen I and III corresponded well with the results in pregnant rat and mouse myometrium near term (Shynlova *et al.*, 2004; Ouellette *et al.*, 2022). Collagen V, which is essential for the fibrillation of collagen I and III and promotes ECM remodeling

(Mak *et al.*, 2016), also showed a significant decline in this study. The collagens degraded in the laboring myometrium as they did in the cervix (Akins *et al.*, 2011). Collagen degradation may be due to the elevation of proteases, including MMPs, which are regulated by various factors such as mechanical tension, inflammation, and hypoxia. This degradation may create a more appropriate microenvironment for cellular contraction and prepare for collagen reorganization after parturition.

Cell adhesion was indicated as another enriched cluster after TIMP1 knockdown in this study. In the rat myometrium, focal adhesion signaling was found to abruptly terminate with the onset of labor (Macphee and Lye, 2000). This phenomenon is possibly associated with mechanical stretch, hormones, and ECM reorganization (Macphee and Lye, 2000; Shynlova *et al.*, 2007; Burkin *et al.*, 2013) and is suggested to help develop optimal contractile activity in laboring. Our findings were in line with these elegant studies showing that cell adhesive capacity is attenuated in laboring hMSMCs. Conversely, knockdown of TIMP1 enhanced cell adhesive capacity and the expression of associated molecules. It is important to note that the attenuated cell adhesive capacity in laboring hMSMCs in this study may mainly be due to the downregulation of adhesion-associated molecules since the changed ECM cannot be fully involved in the cell adhesion assay. ECM, including but not limited to collagens, also influences cell adhesion (Wang *et al.*, 2018). Mice lacking decorin and biglycan were reported to develop dystocia during parturition by Lechner's team (Wu *et al.*, 2012). Conditional deletion of Adamts9 led to reduced VCAN proteolysis and resulted in parturition defects in mice (Mead *et al.*, 2018). In the current study, we observed an increased ratio of MMPs to TIMPs, which led to degraded collagens and attenuated cell adhesive capacity and finally resulted in impaired contraction of the myometrium. The changes in collagens and cell adhesion may both be adaptive to facilitate and coordinate myometrial contraction because contractility and adhesion are thought to be two opposing mechanical forces (Barnhart *et al.*, 2015).

In the current study, we revealed a novel role of TIMP1 in facilitating and coordinating myometrial contraction during human labor. However, there are some limitations. The myometrium is composed of various cells and ECM, and the processes of collagen reorganization and ECM remodeling are complex, involving over 700 proteins. TIMP1, as a single molecule within this intricate network, may only partially regulate these processes. Additionally, TIMP1 itself is pleiotropic and can be influenced by various factors such as hormones, stretch, and immunity, which were not fully elucidated in this study.

Conclusion

The current study indicates that upregulated TIMP1 facilitates and coordinates myometrial contraction by decreasing collagens and cell adhesive capacity during human labor. These findings highlight that the optimal contractile function of the myometrium, which is composed of hMSMCs, infiltrated inflammatory cells, ECM and other possible components, requires the cooperation of a variety of interacting factors. Therefore, a better understanding of these factors will aid in developing new therapeutics to regulate pathological uterine contraction.

Supplementary data

Supplementary data are available at *Molecular Human Reproduction* online.

Data availability

All data generated or analyzed during this study are included in this published article [and its supplementary information files]. The RNA sequencing data can be obtained from the Genome Sequence Archive (GSA) (https://ngdc.cncb.ac.cn/gsa-human/browse/HRA003324).

Acknowledgements

We thank Di Mao, Yuou Chen, Wenfeng Deng, Fan Yang, Bo Li, and Rong Liu for collecting samples and the clinical staff of Guangzhou Women and Children's Medical Center for their assistance.

Authors' roles

H.L., J.B., and X.W. designed research; X.W., J.B., B.W., Q.G., X.P., and Y.C. performed research; K.J., L.C., and J.B. analyzed data; and J.B., L.C., and H.L. wrote the paper. All authors read and approved the submitted version.

Funding

This study was supported by Guangzhou Municipal Science and Technology Bureau grant 20210201040113 (to H.L.), 202201020623 (to X.P.) and 202201020592 (to Z.Z.).

Conflict of interest

All authors declare that there are no conflicts of interest.

References

Akins ML, Luby-Phelps K, Bank RA, Mahendroo M. Cervical softening during pregnancy: regulated changes in collagen cross-linking and composition of matricellular proteins in the mouse. *Biol Reprod* 2011;**84**:1053–1062.

Arpino V, Brock M, Gill SE. The role of TIMPs in regulation of extracellular matrix proteolysis. *Matrix Biol* 2015;**44–46**:247–254.

Baker AH, Edwards DR, Murphy G. Metalloproteinase inhibitors: biological actions and therapeutic opportunities. *J Cell Sci* 2002;**115**:3719–3727.

Bao J, Liu Y, Yang J, Gao Q, Shi SQ, Garfield RE, Liu H. Nicotine inhibits LPS-induced cytokine production and leukocyte infiltration in rat placenta. *Placenta* 2016;**39**:77–83.

Barnett SD, Asif H, Buxton ILO. Novel identification and modulation of the mechanosensitive Piezo1 channel in human myometrium. *J Physiol* 2023;**601**:1675–1690.

Barnhart E, Lee KC, Allen GM, Theriot JA, Mogilner A. Balance between cell-substrate adhesion and myosin contraction determines the frequency of motility initiation in fish keratocytes. *Proc Natl Acad Sci USA* 2015;**112**:5045–5050.

Bockelman C, Beilmann-Lehtonen I, Kaprio T, Koskensalo S, Tervahartiala T, Mustonen H, Stenman UH, Sorsa T, Haglund C. Serum MMP-8 and TIMP-1 predict prognosis in colorectal cancer. *BMC Cancer* 2018;**18**:679.

Burkin HR, Rice M, Sarathy A, Thompson S, Singer CA, Buxton IL. Integrin upregulation and localization to focal adhesion sites in pregnant human myometrium. *Reprod Sci* 2013;**20**:804–812.

Cabral-Pacheco GA, Garza-Veloz I, Castruita-De la Rosa C, Ramirez-Acuna JM, Perez-Romero BA, Guerrero-Rodriguez JF, Martinez-Avila N, Martinez-Fierro ML. The roles of matrix

metalloproteinases and their inhibitors in human diseases. *Int J Mol Sci* 2020;**21**:9739.

Chen L, Wang L, Luo Y, Huang Q, Ji K, Bao J, Liu H. Integrated proteotranscriptomics of human myometrium in labor landscape reveals the increased molecular associated with inflammation under hypoxia stress. *Front Immunol* 2021;**12**:722816.

Fan Y, Hou W, Xing Y, Zhang L, Zhou C, Gui J, Xu P, Wang A, Fan X, Zeng X *et al.* Peptidomics analysis of myometrium tissues in term labor compared with term nonlabor. *J Cell Biochem* 2020;**121**: 1890–1900.

Geng J, Huang C, Jiang S. Roles and regulation of the matrix metalloproteinase system in parturition. *Mol Reprod Dev* 2016;**83**:276–286.

Humphrey JD, Dufresne ER, Schwartz MA. Mechanotransduction and extracellular matrix homeostasis. *Nat Rev Mol Cell Biol* 2014; **15**:802–812.

Jabłońska-Trypuć A, Matejczyk M, Rosochacki S. Matrix metalloproteinases (MMPs), the main extracellular matrix (ECM) enzymes in collagen degradation, as a target for anticancer drugs. *J Enzyme Inhib Med Chem* 2016;**31**:177–183.

Jayes FL, Liu B, Feng L, Aviles-Espinoza N, Leikin S, Leppert PC. Evidence of biomechanical and collagen heterogeneity in uterine fibroids. *PLoS One* 2019;**14**:e0215646.

Kao KY, Leslie JG. Polymorphism in human uterine collagen. *Connect Tissue Res* 1977;**5**:127–129.

Khader N, Shchuka VM, Shynlova O, Mitchell JA. Transcriptional control of parturition: insights from gene regulation studies in the myometrium. *Mol Hum Reprod* 2021;**27**:gaab024.

Kim KH, Burkhart K, Chen P, Frevert CW, Randolph-Habecker J, Hackman RC, Soloway PD, Madtes DK. Tissue inhibitor of metalloproteinase-1 deficiency amplifies acute lung injury in bleomycin-exposed mice. *Am J Respir Cell Mol Biol* 2005;**33**: 271–279.

Li WJ, Lu JW, Zhang CY, Wang WS, Ying H, Myatt L, Sun K. PGE2 vs PGF2alpha in human parturition. *Placenta* 2021;**104**:208–219.

Lombardi A, Makieva S, Rinaldi SF, Arcuri F, Petraglia F, Norman JE. Expression of matrix metalloproteinases in the mouse uterus and human myometrium during pregnancy, labor, and preterm labor. *Reprod Sci* 2018;**25**:938–949.

Lucovnik M, Trojner Bregar A, Bombac L, Gersak K, Garfield RE. Effects of vaginal progesterone for maintenance tocolysis on uterine electrical activity. *J Obstet Gynaecol Res* 2018;**44**: 408–416.

Lv Z, Xiong LL, Qin X, Zhang H, Luo X, Peng W, Kilby MD, Saffery R, Baker PN, Qi HB. Role of GRK2 in trophoblast necroptosis and spiral artery remodeling: implications for preeclampsia pathogenesis. *Front Cell Dev Biol* 2021;**9**:694261.

Ma X, Zhao P, Wakle-Prabagaran M, Amazu C, Malik M, Wu W, Wang H, Wang Y, England SK. Microelectrode array analysis of mouse uterine smooth muscle electrical activity. *Biol Reprod* 2020;**102**: 935–942.

Macphee DJ, Lye SJ. Focal adhesion signaling in the rat myometrium is abruptly terminated with the onset of labor. *Endocrinology* 2000; **141**:274–283.

Mak KM, Png CYM, Lee DJ. Type V Collagen in Health, Disease, and Fibrosis. *Anat Rec (Hoboken)* 2016;**299**:613–629.

Manase K, Endo T, Chida M, Nagasawa K, Honnma H, Yamazaki K, Kitajima Y, Goto T, Kanaya M, Hayashi T *et al.* Coordinated elevation of membrane type 1-matrix metalloproteinase and matrix metalloproteinase-2 expression in rat uterus during postpartum involution. *Reprod Biol Endocrinol* 2006;**4**:32.

Mead TJ, Du Y, Nelson CM, Gueye NA, Drazba J, Dancevic CM, Vankemmelbeke M, Buttle DJ, Apte SS. ADAMTS9-regulated pericellular matrix dynamics governs focal adhesion-dependent smooth muscle differentiation. *Cell Rep* 2018;**23**:485–498.

Nadeem L, Shynlova O, Matysiak-Zablocki E, Mesiano S, Dong X, Lye S. Molecular evidence of functional progesterone withdrawal in human myometrium. *Nat Commun* 2016;**7**:11565.

Nguyen TT, Shynlova O, Lye SJ. Matrix metalloproteinase expression in the rat myometrium during pregnancy, term labor, and postpartum. *Biol Reprod* 2016;**95**:24–14.

Noble NA, Harper JR, Border WA. In vivo interactions of TGF-beta and extracellular matrix. *Prog Growth Factor Res* 1992;**4**:369–382.

Nothnick WB. Disruption of the tissue inhibitor of metalloproteinase-1 gene results in altered reproductive cyclicity and uterine morphology in reproductive-age female mice. *Biol Reprod* 2000;**63**: 905–912.

O'Brien M, O'Shaughnessy D, Ahamide E, Morrison JJ, Smith TJ. Differential expression of the metalloproteinase MMP3 and the alpha5 integrin subunit in human myometrium at labour. *Mol Hum Reprod* 2007;**13**:655–661.

Ouellette A, Mahendroo M, Nallasamy S. Collagen and elastic fiber remodeling in the pregnant mouse myometrium. *Biol Reprod* 2022;**107**:741–751.

Owen CA, Hu Z, Barrick B, Shapiro SD. Inducible expression of tissue inhibitor of metalloproteinases-resistant matrix metalloproteinase-9 on the cell surface of neutrophils. *Am J Respir Cell Mol Biol* 2003;**29**: 283–294.

Owen CA, Hu Z, Lopez-Otin C, Shapiro SD. Membrane-bound matrix metalloproteinase-8 on activated polymorphonuclear cells is a potent, tissue inhibitor of metalloproteinase-resistant collagenase and serpinase. *J Immunol* 2004;**172**:7791–7803.

Oxlund BS, Ortoft G, Bruel A, Danielsen CC, Bor P, Oxlund H, Uldbjerg N. Collagen concentration and biomechanical properties of samples from the lower uterine cervix in relation to age and parity in non-pregnant women. *Reprod Biol Endocrinol* 2010;**8**:82.

Pique-Regi R, Romero R, Garcia-Flores V, Peyvandipour A, Tarca AL, Pusod E, Galaz J, Miller D, Bhatti G, Para R *et al.* A single-cell atlas of the myometrium in human parturition. *JCI Insight* 2022;**7**: e153921.

Prideaux M, Staines KA, Jones ER, Riley GP, Pitsillides AA, Farquharson C. MMP and TIMP temporal gene expression during osteocytogenesis. *Gene Expr Patterns* 2015;**18**:29–36.

Rabotti C, Mischi M. Propagation of electrical activity in uterine muscle during pregnancy: a review. *Acta Physiol (Oxf)* 2015;**213**:406–416.

Read CP, Word RA, Ruscheinsky MA, Timmons BC, Mahendroo MS. Cervical remodeling during pregnancy and parturition: molecular characterization of the softening phase in mice. *Reproduction* 2007;**134**:327–340.

Shynlova O, Mitchell JA, Tsampalieros A, Langille BL, Lye SJ. Progesterone and gravidity differentially regulate expression of extracellular matrix components in the pregnant rat myometrium. *Biol Reprod* 2004;**70**:986–992.

Shynlova O, Williams SJ, Draper H, White BG, MacPhee DJ, Lye SJ. Uterine stretch regulates temporal and spatial expression of fibronectin protein and its alpha 5 integrin receptor in myometrium of unilaterally pregnant rats. *Biol Reprod* 2007;**77**:880–888.

Stetler-Stevenson WG. Tissue inhibitors of metalloproteinases in cell signaling: metalloproteinase-independent biological activities. *Sci Signal* 2008;**1**:re6.

Stewart EA, Floor AE, Jain P, Nowak RA. Increased expression of messenger RNA for collagen type I, collagen type III, and fibronectin in myometrium of pregnancy. *Obstet Gynecol* 1995;**86**:417–422.

Timmons B, Akins M, Mahendroo M. Cervical remodeling during pregnancy and parturition. *Trends Endocrinol Metab* 2010;**21**: 353–361.

Wang H, Lafdil F, Wang L, Yin S, Feng D, Gao B. Tissue inhibitor of metalloproteinase 1 (TIMP-1) deficiency exacerbates carbon tetrachloride-induced liver injury and fibrosis in mice: involvement of hepatocyte STAT3 in TIMP-1 production. *Cell Biosci* 2011; **1**:14.

Wang X, Rojas-Quintero J, Wilder J, Tesfaigzi Y, Zhang D, Owen CA. Tissue inhibitor of metalloproteinase-1 promotes polymorphonuclear neutrophil (PMN) pericellular proteolysis by anchoring matrix metalloproteinase-8 and -9 to PMN surfaces. *J Immunol* 2019;**202**:3267–3281.

Wang Z, Li R, Zhong R. Extracellular matrix promotes proliferation, migration and adhesion of airway smooth muscle cells in a rat model of chronic obstructive pulmonary disease via upregulation of the PI3K/AKT signaling pathway. *Mol Med Rep* 2018;**18**: 3143–3152.

Wen B, Zheng Z, Wang L, Qian X, Wang X, Chen Y, Bao J, Jiang Y, Kaiyuan JI, Liu H. HIF-1alpha is essential for the augmentation of myometrial contractility during labor. *Biol Reprod* 2022;**107**: 1540–1550.

Winkler M, Fischer DC, Ruck P, Marx T, Kaiserling E, Oberpichler A, Tschesche H, Rath W. Parturition at term: parallel increases in interleukin-8 and proteinase concentrations and neutrophil count in the lower uterine segment. *Hum Reprod* 1999a;**14**: 1096–1100.

Winkler M, Oberpichler A, Tschesche H, Ruck P, Fischer DC, Rath W. Collagenolysis in the lower uterine segment during parturition at term: correlations with stage of cervical dilatation and duration of labor. *Am J Obstet Gynecol* 1999b;**181**:153–158.

Wu Z, Aron AW, Macksoud EE, Iozzo RV, Hai CM, Lechner BE. Uterine dysfunction in biglycan and decorin deficient mice leads to dystocia during parturition. *PLoS One* 2012;**7**:e29627.

Yu Q, Stamenkovic I. Cell surface-localized matrix metalloproteinase-9 proteolytically activates TGF-beta and promotes tumor invasion and angiogenesis. *Genes Dev* 2000;**14**:163–176.